

## Characterization of 3D Printed PLA/PCL/TiO<sub>2</sub> Composites for Cancellous Bone

Nájera S<sup>1</sup>, Michel M<sup>1</sup>, Kyung-Hwan J<sup>2,3</sup> and Nam-Soo Kim<sup>1\*</sup>

<sup>1</sup>Department of Metallurgical, Materials and Biomedical Engineering, Printing Nano Engineering Laboratory, The University of Texas at El Paso, El Paso, Texas 79968, USA

<sup>2</sup>Korea Institute of Industrial Technology, Gangwon Regional Division, Gangneung 25440, Republic of Korea

<sup>3</sup>KIMM Metal 3D Printing Convergence Research Team, Daejeon 34103, Republic of Korea

### Abstract

The reproduction of a 3D bone structure with suitable porosity, which allows the flow of nutrients, blood, oxygen and mineral, remains a problem using conventional methods. A material that mimics their properties was developed by optimizing the ratio of a biodegradable blend of immiscible polylactic acid (PLA) and poly-ε-caprolactone (PCL). In this study, PLA and PCL particularly optimize the strength of the artificial cancellous bone by supplying the initial support strength lasting 6 months to 2 years and allowing for the gradual degradation desired in the human body. This study focused on the mechanical properties of successfully printed 3D structures. The ultimate tensile strength was modified by blending different ratios of PLA and PCL resulting in an optimum value of approximately 30 MPa when the ratio of PLA to PCL reached 3:1. The addition of 1 wt.% of titanium dioxide (TiO<sub>2</sub>) to the immiscible PLA/PCL composite and the modification of the interface area between them resulted in the formation of a binding force that allowed for an increase in the tensile strength up to 37 MPa. Besides the mechanical properties, the in vitro biocompatibility of PLA/PCL/TiO<sub>2</sub> composites was examined. A vigorous cell growth was observed in the cells cultivated with the PLA/PCL/TiO<sub>2</sub> composites and the unimpeded ability to differentiate into osteoblast also was found. The resulting properties of the 3D printed structures indicate promising applications in the fields of bone tissue engineering and cancellous bone grafting.

**Keywords:** Polylactic acid; Polycaprolactone; TiO<sub>2</sub>; Interface area; 3D printing; Bone tissue; Porosity; Biocompatibility

### Introduction

Bone grafting is beneficial to repair bones that have been severely damaged or have been lost. Diseases such as arthritis, traumatic injury, and surgery for bone tumor became very common in the senior population, and this has spotlighted and augmented the research into the design of new materials to expand their application. Bone replacement may be classified as permanent or temporary depending on the characteristics of its material. A permanent replacement is used when a bone is missing and a temporary implant is used when the implant will be removed after the treatment is successful [1]. The choice of bone graft depends on varying considerations including the intended clinical application, defect size, mechanical properties, availability, required bioactivity (osteoconductive/osteoinductive/osteogenic), handling problem, cost and ethical issues [2]. Once these issues have been considered, the types of grafts can be classified as autograft, allograft and bone graft substitutes, each with its own advantages and disadvantages. Autograft and allograft depend to great extent on the suitability of the donor and constitute essentially the positioning of bones from one place or person, to another. Bone graft substitutes require specific material characteristics and are the subjects of a multitude of studies that focus on engineering substitutes or scaffolds to support bone tissue. The ultimate tensile strength (UTS) and Young's Modulus of human bones are 60 ~ 120 MPa for compact bones and 7~25 GPa respectively at different ages [2,3]. The concept of bone tissue engineering includes the design and building of a synthetic frame that will mimic the mechanical properties of the bone. This scaffold should combine mechanical function and tissue generation. Since bones are not homogenous, but formed by bone tissue that varies in composition and porosity, the scaffolds that will support or replace them should be adequately designed [4]. The mechanical properties depend upon the porosity, size and distribution of hydroxyapatite (HA) crystals within collagen fibrils, and the presence and distribution

of micro cracks within the bone. The collagen fibril matrix provides both toughness and tensile strength and the crystalline HA structure provides compressive strength and brittleness. Because of this, the optimization of porosity needs to mimic the superficial cortical (high density tissue) and the internal cancellous (more porous) bones. The mechanical and biological performance of scaffolds depends on the integration of the computational topology design, the solid free form fabrication and the material used to fabricate it [5,6]. To initiate the development of materials for bone grafting, the scaffolds should be fabricated, then tested for their mechanical characteristics and, beyond that fabricated scaffolds needed to be validated as appropriate candidates to be used in animals as well as in the human body.

The process of grafting is expensive because it usually includes metal substitutes such as stainless steel, magnesium, titanium or cobalt alloys, and this method of using metal has had some problems due to factors such as the metal's higher strength and toxicity. Some kinds of metal ions (titanium, aluminum, vanadium, nickel, cobalt, chromium) released over a period of time are toxic in the human body, and even if some of them are normal components of the body, they can become toxic at high dosage [7]. When the strength of the bone is less than the transplanted support, the bone will most likely

**\*Corresponding author:** Nam-Soo Kim, Department of Metallurgical, Materials and Biomedical Engineering, The University of Texas at El Paso, 500 W University Ave, El Paso, TX 79968, USA, Tel: +1 915-747-7996; Fax: +1 915-747-8036; E-mail: [nkim@utep.edu](mailto:nkim@utep.edu)

**Received** January 27, 2017; **Accepted** February 02, 2018; **Published** February 12, 2018

**Citation:** Nájera S, Michel M, Kyung-Hwan J, Nam-Soo K (2018) Characterization of 3D Printed PLA/PCL/TiO<sub>2</sub> Composites for Cancellous Bone. J Material Sci Eng 7: 417. doi: [10.4172/2169-0022.1000417](https://doi.org/10.4172/2169-0022.1000417)

**Copyright:** © 2018 Nájera S, et al. This is an open-access article distributed under the terms of the Creative Commons Attribution License, which permits unrestricted use, distribution, and reproduction in any medium, provided the original author and source are credited.

break instead of the implant, since the implant carries most of the load resulting in a weakening of bone (stress shielding). For these reasons, temporary grafting is preferred, eliminating or replacing it as needed. Biodegradable materials have emerged to solve these problems [8]. Taking advantage of the regenerative character of bones, implants or grafts no longer need to be removed thus minimizing trauma and risks of infection from secondary surgeries. The biodegradable scaffold can degenerate and eventually disappear as new tissue is growing and regenerating. Biodegradable magnesium alloys, ceramics and polymers make suitable scaffold building materials. Currently used biodegradable polymers include polylactic acid (PLA), polyglycolic acid (PGA), poly-ε-caprolactone (PCL) and poly-β-hydroxybutyrate (PHB) as well as polylactic acid-ε-glycolic acid (PLGA) [9].

Polymer based biodegradable materials are categorized as natural and synthetic. Both have been used for medical applications [10-12]. Collagen, chitosan, gelatin, fibrin and hyaluronic acid are natural biodegradable polymers. PLA and PCL are synthetic biodegradable thermoplastic polymers, and are prominently used as a main material because they can be used in the human body for surgery [13,14]. PLA and PCL have been used in the field of biomedical applications due to their biocompatibility with the human body, and their mechanical properties *in vivo*. Specific properties can be obtained when different polymers are mixed and can be tailored depending on the application in which they will be used. PLA can be blended with other flexible polymers that will act as plasticizers to improve its toughness and reduce its brittleness [15]. PCL is a biocompatible and biodegradable aliphatic polyester like PLA. It has good toughness, displays rubbery properties and has low glass transition and melting temperatures. It is also more thermally stable than PLA, which opens the possibility that the presence of PCL in PLA will not only improve its toughness, but also its thermal stability. When it is blended with PCL, the brittleness of PLA is improved [16]. The possibility of the application of these two polymers as bone graft scaffolds and biomaterials is growing since they complement each other in their physical properties and biodegradability. Titanium dioxide (TiO<sub>2</sub>) particles can be introduced into the composite to obtain even more favorable material properties such as toughness, flexibility and thermal stability [17]. Although TiO<sub>2</sub> is an inorganic particle, it exhibits suitable biocompatibility and is well known to be non-toxic depending on the size of the particles and condition of aggregation [18,19]. In addition to all these properties, titania, with its antibacterial characteristics [20], helps reduce the risk of infections from implants in the body. The TiO<sub>2</sub> can serve as filler for additional reinforcement and to increase the polymer's mechanical properties. The addition of TiO<sub>2</sub> into the materials requires the particles to be scattered uniformly into the blend to prevent bulging of the material [21].

Additive layer manufacturing (ALM) involves the computer-generated model or computer aided design (CAD) of the desired object and then, the rapid prototyping that includes the solid freeform fabrication (SFF) of such design through one of the different ALM techniques. Stereolithography (SL), digital light processing (DLP), selective laser sintering (SLS), fused deposition modeling (FDM), and multi jet modeling (MJM) are some of the methods used. FDM is a 3D printing process that builds structures by extruding a semiliquid thermoplastic filament layer by layer. When the materials used for printing have the property of a thermoplastic, the dispenser is able push the material out. This method has various advantages, the equipment and maintenance costs being low since the structures and devices of the program are simple compared to other printing techniques. For example, with the help of RepRap (Replicating Rapid-prototyper),

which is an open source rapid prototyping system, the replication of printer parts can be made and thus the technique applied to a variety of materials. Furthermore, when the precision of the controlling device is augmented, it can be applied to a wider range of industries to strengthen the surface roughness of the models. FDM can build complex structures, open or closed cell and this makes it possible to build a structure in which biological components can be incorporated thus allowing for the regeneration of the bone. Since the building material can be developed as a spooled precursor rod before being extruded, it is possible to create polymer matrix composite materials with suspended particles, including nanoparticles within the matrix. The complex nature of the bones with its different porosity areas (cortical and cancellous) can thus be recreated by 3D printing.

In the present study, we propose a suitable polymer blend composite through the optimization of the mechanical properties and by later being integrated with biological components of the innate bone such as collagen. We found the optimum mechanical properties when the PLA and PCL were blended at a ratio of 3:1. Moreover, the addition of 1 wt.% of titanium dioxide results in a comparable mechanical strength of the ideal cancellous bone structure.

## Materials and Methods

### Materials

The polylactic acid used in the study was a commercial grade (PLA 4043D), with a density of 1.24 g/cc, glass transition temperature of ~53°C and a melting temperature of ~153°C. The polycaprolactone (Sigma-Aldrich, St. Louis, MO) has a density of 1.15 g/cc at 25°C, a glass transition temperature of ~60°C and a melting temperature ~65°C. The titanium dioxide (Sigma-Aldrich, St. Louis, MO) was received as anatase with a melting point of >350°C, and a density of 4.26 g/cc at 25°C, and the particles size varied from 0.5 to 1 µm.

### Filament preparation

To make the filament, a blend was prepared to make pellets with the desired composition. The first blends made were a mixture of PLA/PCL with different compositions (75/25 wt.%, 50/50 wt.% and 25/75 wt.% PCL). After testing their mechanical properties, the blend composed of 75 wt.% PLA and 25 wt.% PCL showed the best characteristics. This composition was the one selected to study the effect of the addition of titanium dioxide. The mixing process starts by first melting the corresponding amount of PLA due to its higher melting point. PCL is then added, and when the blend is uniformly mixed, the filler is added and stirred until a homogeneous mixture is achieved. The solid mixture is then cut into pieces small enough to be fed into the filament extruder (Figure 1). This extruder was developed by Maker's Station Inc. (El Paso, TX).

### Structure fabrication

The biomaterial filaments made of various compositions of PLA, PCL and TiO<sub>2</sub> were introduced into a 3D printer. For this investigation, fused deposition modeling was used to print specimens for tensile testing, according to the standards of the American Society for Testing and Materials (ASTM) D638 type IV, and outer structure of the artificial bone (Figure 2). This method works by continuous addition of thin layers of material. The filament is placed into the heated extruder and according to the 3D data the material is extruded through a nozzle to 3D print the cross section of the desired object into a heated platform. The melted filament layers will bond to the previous layers as they solidify. The printing process for all different filaments used the

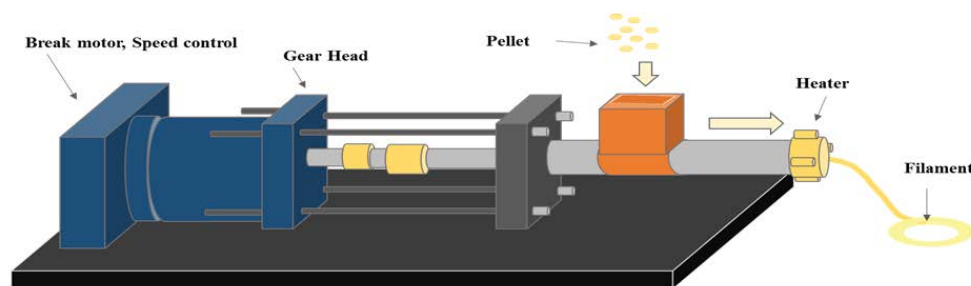


**Figure 1:** Schematic diagram of the filament extruder used for blending and making PLA/PCL filaments.



**Figure 2:** 3D printed model of cancellous bone with PLA/PCL/TiO<sub>2</sub> 74.25/24.75/1 wt.% composite.

same or very similar conditions to print. Tensile samples used to test the polymer-polymer interface were made using a similar printer but with two nozzle heads instead of one. The process is the same, only the code is modified so that the printer alternates between two different nozzles, each with its own filament, using only one extruder at a time, controlling different temperatures and printing speeds. The quality of the final print is dependent on the temperature, speed and the layer thickness. The printing process for all different filaments uses the same or very similar conditions to print.

### Analysis tools

**Differential scanning calorimetry (DSC):** The heat flow of the composites was analyzed by differential scanning calorimetry (DSC 404 F1 Pegasus, NETZSCH, Germany) to confirm whether PLA and PCL exhibit miscible or immiscible behavior. The scan speed was constant at 5°C/min by using controlled mixed gases. The setting temperature of the blended PLA/PCL and PLA/PCL/TiO<sub>2</sub> was determined by following the DSC results.

**Tensile testing:** Tensile testing is used to see how samples behave under load, and to define the material as brittle or ductile. A Mark-10 ESM301/ESM301L Motorized Test Stand was used to perform the test for all samples. All the tests were conducted at room temperature.

**Scanning electron microscope (SEM):** To observe the fracture surface of the composites SEM was adopted. SEM uses a beam of electrons to generate signals at the surface of solid specimens and it is able to show the texture and the chemical composition of the sample. The samples were cut parallel to the fracture surface having a height of approximately 5 mm. They were mounted on the holder using double-sided conductive carbon tape; no coating was needed to examine the specimens. The scanning electron microscope used in this work was a Hitachi Tabletop TM-1000 with an accelerating voltage of 15 kV.

### Interface analysis

A polymer blend interface is when a polymer is in contact with another polymer and a polymer composite interface when it is in

contact with filler or other non-polymer materials. The blends of PLA and PCL are immiscible because of the resulting low entropy and the heat of mixing which is frequently positive [22]. According to Helfand and Tagami, an interface is when the molecular species occupy a space of a very small length, and the composition in these phases varies [23]. The interface area of two polymers increases when they are mixed in powder state. Since in this work PLA and PCL were melt mixed, they have a low interface, but much higher than the samples made using a dual nozzle head. The mechanical behavior between different interfaces can be described in terms of thermodynamics. Tensile strength samples were designed to get the same 50:50 ratio with different number of interfaces. This ratio was chosen because at this point the samples would have the maximum value of  $\Delta S$ . To study the effects of interface areas, the overlapping gauge was changed as illustrated in below figure. When the number of interfaces is higher, the interface area increases dramatically. In this study, the change in tensile strength was studied according to the change (increase) in the interface area.

### Biocompatibility test

**Cell culture:** Mouse calvarial isolated preosteoblast cell line, MC3T3-E1 subclone 4 were grown in alpha-MEM (Gibco, Gran Island, NY) supplemented with 10% fetal bovine serum 100 U/ml penicillin, and 100 µg/ml streptomycin (Gibco, Gran Island, NY) under a humidified atmosphere of 95% air/5% CO<sub>2</sub> at 37°C. Cells were subcultured 2-3 times per week, and the medium was changed every other day. To induce osteoblast, cells were cultured in  $\alpha$ -MEM containing 50 mg/L of ascorbic acid, 10 mM  $\beta$ -glycerophosphate, and 50 ng/ml of BMP2 (Sigma-Aldrich, Sr. Louis, MO). All the PLA/PCL/TiO<sub>2</sub> composites were sterilized with 2X antibiotics solution (2% penicillin and streptomycin) for 1 hour at room-temperature and pre-incubated in growth medium for 3 additional hours at 37°C.

**Cell proliferation assay:** Cell proliferation assay was performed using Celltiter 96<sup>®</sup> aqueous one solution cell proliferation assay (Promega, Madison, WI) according to the manufacturer's instructions. Cells were seeded in the 96-well culture plate at  $1 \times 10^3$  cells/well with PLA/PCL/TiO<sub>2</sub> composites. At days 1, 3, 5, 7 and 14 a 10 µl/well of MTS reagent was added for 2 hours at 37°C to allow the formation of a soluble violet formazan product by viable cells. MTS-1 reagent is a stable tetrazolium salt. When it is cleaved into soluble formazan by a dehydrogenase such as succinate-tetrazolium reductase, it detects only viable cells. Therefore, the optical density of violet formazan dye is correlated directly to the number of cells. The absorbance was determined to be 490 nm using a microplate spectrophotometer (BioTek, Winooski, VT).

**Immunofluorescence:** Cells were cultured onto a 12-well culture plate at a density of  $1 \times 10^4$  cells/well in the PLA/PCL/TiO<sub>2</sub> composites



or a poly-D-lysine coated coverslip. For filamentous-actin staining, cells were washed with PBS and fixed with 10% neutral buffered formalin (Sigma-Aldrich, Sr. Louis, MO) for 15 min. Cells were then treated with 0.1% Triton X-100 for 5 min at room temperature and reacted with Rhodamine-conjugated phalloidin (Molecular Probe, Eugene, Oregon) for 2 hours at room temperature. To protect the fluorescence signals and make the nuclei visible, cells were mounted with DAPI containing mounting solution (Vector Laboratories, Burlingame, CA). All fluorescence images were captured by a LSM 700 confocal microscope (ZEISS, Jena, Germany).

**Alkaline phosphatase (ALP) and alizarin red S staining:** For ALP staining, MC3T3-E1 cells were cultured in 48-well culture plate at a density of  $1 \times 10^5$  cells/well. After osteoblast differentiation using conditioned medium, alkaline phosphatase staining was performed using Leukocyte alkaline phosphatase kit (Sigma-Aldrich, Sr. Louis, MO) according to the instruction. Cells were immersed in a fixative solution (2.5 ml of citric acid, 6.5 ml of acetone and 0.8 ml of 37% formaldehyde) for 1 min, rinsed with distilled water, and incubated with Naphthol-AS-BL alkaline solution mixture at room-temperature for 30 min. Cells were additionally rinsed with distilled water and air dry. For alizarin red S staining, cells were plated in 48-well culture plate at a density of  $1 \times 10^5$  cells/well. After being fixed in 10% neutral buffered formalin for 15 min at room temperature, cells were rinsed with distilled water and stained with 2% Alizarin Red S solution (Millipore, Billerica, MA) for 30 min, washed again, air dry images were photographed.

**RNA extraction and real-time PCR:** Total RNA was extracted using Trizol reagent (Sigma-Aldrich, Sr. Louis, MO) and cDNA was synthesized by M-MLV reverse-transcriptase (Promega, Madison, WI). To quantify the relative mRNA expression of osteogenic markers, the primer for ALP (forward; 5'-CCAACTCTTTTGCCAGAGA-3', reverse; 5'-GGCTACATTGGTG TTAGCTTTT-3'), osteocalcin (forward; 5'-GCAATAAGGTAGTGAACAGACTCC-3', reverse; GTTT GTAGGCGGTCTTCAAGC-3') and GAPDH (forward; 5'-AGGTC-GGTGTGAACGGATTTG-3', reverse; 5'-TGTAGACCATGTAG TT-GAGGTCA-3') were used. Diluted cDNA by one over two was mixed with  $1 \times$  SYBR green master mix (Applied Biosystems, Foster city, CA) and  $0.2 \mu\text{M}$  forward and reverse primers. Quantitative RT-PCR was performed using StepOne real-time PCR (Applied Biosystems, Foster city, CA) and normalized by GAPDH levels.

## Results and Discussion

### Effect of material composition

**Mechanical behavior of PLA/PCL composites:** To demonstrate the mechanical properties of PLA/PCL composites, tensile test was performed. Figure 3a represents the stress and strain curves of premixed filament of PLA and PCL. The graph shows the strength of the polymers improving with increasing percentage of PLA. The slope of the strain-stress curves indicates Young's modulus which is the degree of deformation and elongation of the samples when subjected to tensile stress. As the content of PCL increased, the Young's modulus and ultimate strength (UTS) decreased whereas tensile strain was increased. In other words, the composites with higher concentration of PCL are more rigid and have small deformation. The fracture images in Figure 3b consist with the stress and strain curves which show more ductile behavior.

It has been suggested that immiscible blended materials present poor mechanical behaviors, however the weight ratio of PLA/PCL 75/25 wt.% shows the highest tensile stress compared to the other composites. The mechanical properties can be modified depending on the blending process such as melt blending technique [24]. In the present study, it has been proved that the tensile stress and strain can be controlled by the amount of PCL during the blending process.

To confirm the mechanical properties of PLA/PCL composites, we performed the hardness test and found that the hardness was decreased when the amount of PCL was increased (data not shown). However, the hardness of PLA/PCL 75/25 wt.% was increased compared with the weight ratio of PLA/PCL 50/50 wt.%. The hardness can be affected by the porosity within the structure and explains why there is fluctuation in the pattern of hardness.

**Surface analysis of PLA/PCL composites:** Images taken with the SEM show the surface of the specimens from different composition ratios. As shown in Figure 4, there is no spacing on the surface of PLA/PCL blends at the weight ratio of 100/0, 75/25, 25/75 wt.% which means there is good bonding between fibers (Figure 4a-4c). The sample composed of PLA/PCL 75/25 wt.% appears to have a rough surface due to the high mixing energy between these immiscible polymers. On the other hand, the surface of PLA/PCL blends with 0/100 wt.% shows some space between fibers and it may occur by the fixed range of 3D printing temperature from 150°C to 200°C and the fact that the

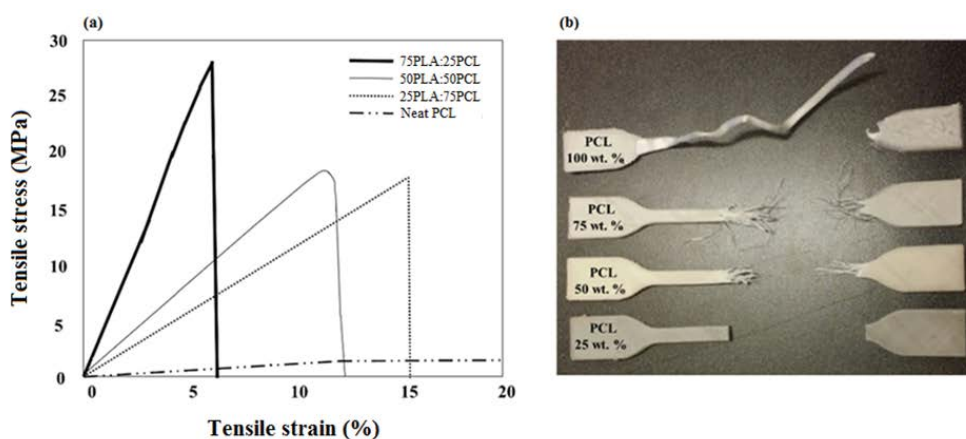


**Figure 3:** (a) Stress-strain curves for different compositions of PLA/PCL, (b) Fracture images corresponding to curves.

materials had been extruded in a liquid state which may cause the structure to shrink as it solidifies (Figure 4d).

### Effect of interface area for PLA/PCL composites

**Mechanical behavior of PLA/PCL interface:** The effect of the different interfaces on the tensile strength is shown in Figure 5. Samples labeled in the figure are composed of PLA/PCL 50/50 wt.%, but with different specific interface areas. Sample A and B were printed using a dual nozzle head printer and they have different interface patterns; sample A has an interface area of 0.2 mm<sup>2</sup>/g, and sample B, 0.7 mm<sup>2</sup>/g. A greater interface area is expected when polymers are melt mixed, and this can be observed in sample C with 24.2 mm<sup>2</sup>/g, assuming the radius cluster of PLA is 100 μm. Larger interface areas enhances stronger adhesion forces that improve the mechanical properties of the blends giving a better reinforcement to the system [25]. The tensile strain shows that the samples with a larger interface area will elongate more. These results demonstrated that tensile strength and modulus are higher when polymers are premixed by using melt blending. The interface between pure PLA and PCL is expected to have the same effects from melt blending technique during the printing process.

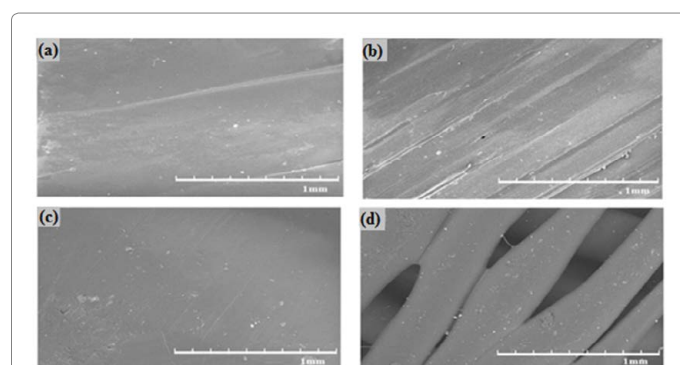


**Figure 4:** Scanning electron microscope (SEM) images of surface area of PLA/PCL composites. (a) PLA/PCL 100/0 wt.%, (b) PLA/PCL 75/25 wt.%, (c) PLA/PCL 25/75 wt.%, and (d) PLA/PCL 0/100 wt.%.

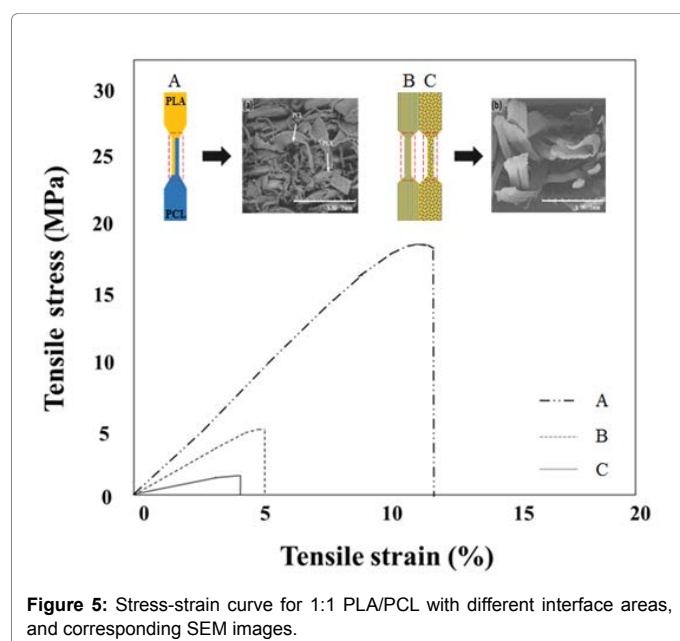


**Figure 5:** Stress-strain curve for 1:1 PLA/PCL with different interface areas, and corresponding SEM images.

**Fractography of PLA/PCL Interface:** The partial rupture of the PLA and PCL for different types of interface can be seen in the SEM images (Figure 5). Images illustrate the position of the fracture plane of the sample with PCL 100 wt.%. When the portion of pure PCL is pulled, it should elongate. On the other hand, the bonding force of PLA holds the PCL and the tension rushes to the relatively weaker parts. Eventually the interfacial strength, which is the weakest part of the PCL will break during the tensile strength test. The samples that were mixed randomly showed a different result-the sample broke along the gauge length. These results also show that the specimen failed at the point of poor interface, and not in the interface line. Also in Figure 5, the SEM image of a dual type specimen shows that the PCL-PLA interfaces lines are not strong enough. Collectively, we demonstrate that tensile strength is better at higher interface numbers in immiscible conditions because it creates stronger bonds along the largest interfaces.

### Effect of TiO<sub>2</sub> in PLA/PCL composites

**Mechanical behavior of PLA/PCL/TiO<sub>2</sub> composite:** To investigate the effect of TiO<sub>2</sub> in the mechanical properties of PLA/PCL composites, tensile strength testing was performed. The tensile strength decreased depending on the amount of TiO<sub>2</sub> as can be observed in Figure 6. As demonstrated in Figure 3, the tensile stress of PLA/PCL blend without TiO<sub>2</sub> has an approximate value of around 28 MPa. The highest tensile strength of the composite was created by mixing with 1 wt.% of TiO<sub>2</sub> and a decrease in strength was observed when the amount of TiO<sub>2</sub> was increased to 3 and 5 wt.%. This is caused by the agglomeration of particles in the polymer matrix implying that the blend needs to be mixed with different methods or use a lower amount of TiO<sub>2</sub> to obtain better performance. Several studies have reported the mechanical properties of PLA/PCL with the tensile strength of 52.9 MPa and 28 MPa for PLA and PCL, respectively and it is consistent with our data which was shown in Figure 3 [26].

**Fractography of PLA/PCL/TiO<sub>2</sub> composite:** The fracture surface morphologies of PLA/PCL and PLA/PCL/TiO<sub>2</sub> composites were studied by scanning electron microscopy as shown in Figure 6b and 6c. It can be observed that TiO<sub>2</sub> particles are evenly dispersed in the PLA/PCL matrix even at a low concentration such as 1 wt.%. The photographic evidence observed in the SEM images correlates to the physical characteristics of the filaments. A brittle fracture surface showing little elongation of fibers and a porous, rough surface is seen in Figure 6b. Contrarily in Figure 6c, a more fibrous fracture surface, indicating the elongation of the filament before breaking. Based on the evidence of images and measured properties, a higher tensile strength is expected in the PLA/PCL/TiO<sub>2</sub> composites.

### Thermal analysis

Differential scanning calorimetry results give us useful information regarding the immiscibility of different types of polymers. Figure 7 shows melting endotherm of PLA and PCL appear at 66°C and 183°C, respectively. For the blend with a 3:1 ratio of PLA and PCL, there are two peaks for the melting temperatures which demonstrate these polymers are immiscible. The presence of PCL in the blend does not affect the melting temperature of the PLA. Crystallization exothermic peaks are located at the range of 90°C to 100°C for the 3:1 mixture meaning that PCL increases the crystallinity. This crystallization behavior is common in PLA, and it controls the degradation rate and the mechanical properties [27]. It has been reported that higher amounts of crystallinity in a material improve its mechanical properties [28]. In addition, the increased stability of the polymers by the addition of TiO<sub>2</sub> has been proved in this study. The particles of TiO<sub>2</sub> have improved the

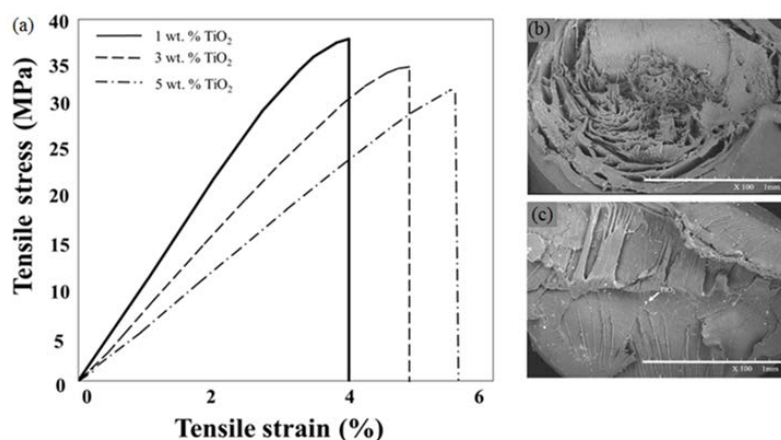


**Figure 6:** Stress-strain curve of PLA/PCL/TiO<sub>2</sub> composites (a), and SEM images of (b) PLA/PCL, (c) PLA/PCL/TiO<sub>2</sub> (arrows indicate TiO<sub>2</sub>).

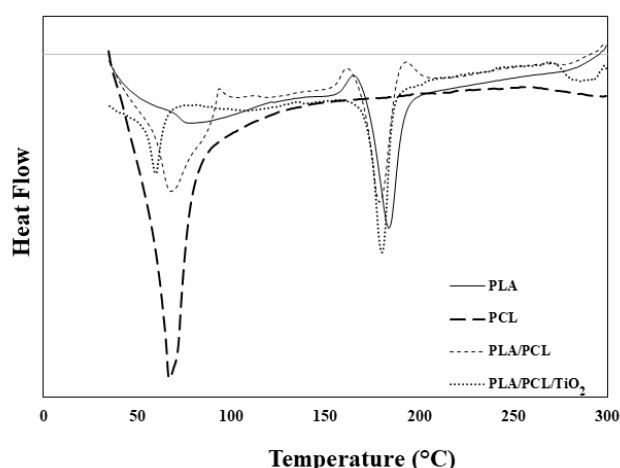


**Figure 7:** Differential scanning calorimetry measurements of PLA 100 wt.%, PLA/PCL 75/25 wt.%, PLA/PCL/TiO<sub>2</sub> 74.25/24.75/1 wt.% and PCL 100 wt.%.

stability of PLA without affecting melting temperature through the enhanced interaction between PLA and the particles.

### ***In Vitro* biocompatibility of PLA/PCL/TiO<sub>2</sub> composite**

To examine the cellular effect of the PLA/PCL/TiO<sub>2</sub> composites, MC3T3-E1 preosteoblast cells were adopted. The cells were seeded onto the PLA/PCL/TiO<sub>2</sub> composites, and the quantitative analysis was performed by cell proliferation assay at 1, 3, 5, 7 and 14 days post-seeding. Figure 8 indicates that the cell growth significantly increased in the PLA/PCL/TiO<sub>2</sub> composites in a time-dependent manner even though no appreciable difference was observed among the types of composites. Consistent with these results, the cells readily adhered and spread out on the surface of all types of PLA/PCL/TiO<sub>2</sub> composite (Figure 9). These data suggest that the PLA/PCL/TiO<sub>2</sub> composite can promote cell growth, and that the composites used for the experiments do not present cytotoxicity through modification of the fabrication process.

Given the robust cell proliferation and adhesion that was observed in PLA/PCL/TiO<sub>2</sub> composites, the effect of PLA/PCL/TiO<sub>2</sub> composites

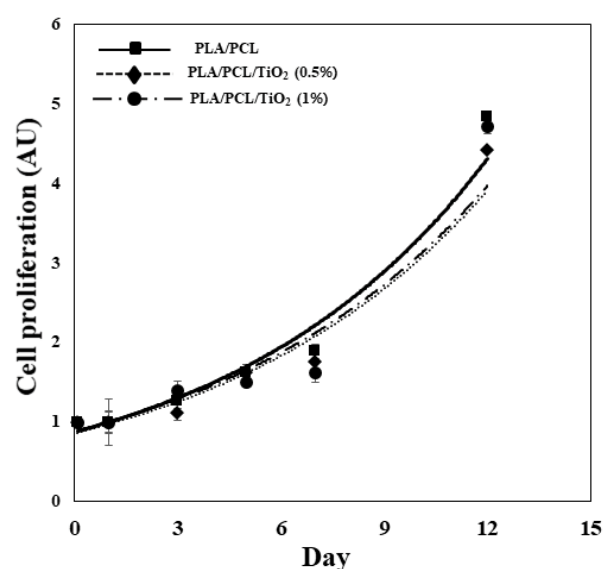


**Figure 8:** Effect of MC3T3-E1 cells proliferation on PLA/PCL/TiO<sub>2</sub> composites. Cell proliferation increased in a time-dependent manner and data did not show significant variation between different types of composites. Results are shown as the mean  $\pm$  SD and  $n \geq 4$  for each point (AU; arbitrary unit).

in osteoblast differentiation was investigated using MC3T3-E1 cells. As shown in Figure 10, the ability of osteoblast differentiation was conducted with different types of PLA/PCL/TiO<sub>2</sub> composites and the disparity among the composites was not found. In addition, the relative mRNA expression of alkaline phosphatase (ALP) and osteocalcin (OCN), which are osteoblastic markers, was examined. The enhanced mRNA expression of ALP and OCN was observed in all the PLA/PCL/TiO<sub>2</sub> composites compared with that of the control (Figure 10c and 10d). It has been suggested that there are variable effects of TiO<sub>2</sub> in osteoblast differentiation depending on the size of particles blending with other materials; however, in our experiments the general tendency was an improved osteoblast differentiation by the addition of TiO<sub>2</sub> particles [29,30].

Taken together, the composites using PLA/PCL/TiO<sub>2</sub> have great biocompatibility including cell proliferation, adhesion and osteoblast



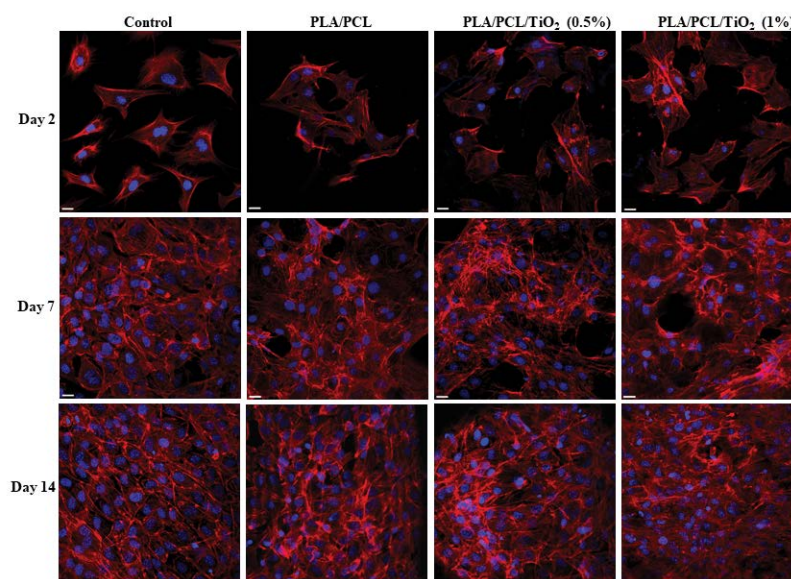


**Figure 9:** Effect of MC3T3-E1 cells adhesion and spreading of PLA/PCL/TiO<sub>2</sub> composites. Filamentous actin structure was observed by rhodamine-conjugated phalloidin and the cells were completely integrated with all types of PLA/PCL/TiO<sub>2</sub> composites (Scale bar; 20  $\mu$ m).

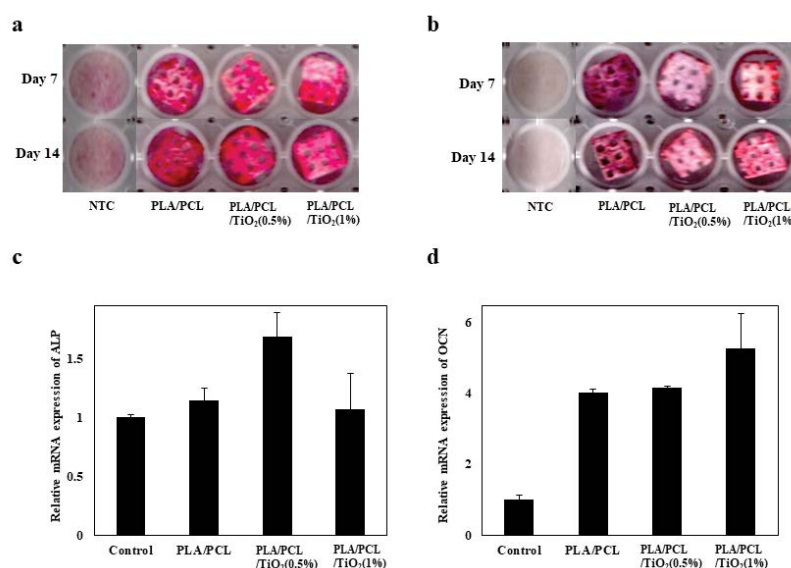


**Figure 10:** Osteoblast differentiation in PLA/PCL/TiO<sub>2</sub> composites. (a) Alkaline phosphatase staining, (b) Alizarin red S staining (c) Relative mRNA expression of osteoblast marker on differentiation day 7 (ALP; alkaline phosphatase, OCN; osteocalcin, NTC; negative control).

differentiation that can improve the new strategy for printing 3D bone structure. To enforce the approach, we proposed the schematic design of 3D structure shown in Figure 11. It displays the original bone structure which is divided into two parts due to the porosity of the bone (Figure 11a). The outer part of the bone, called compact bone, has a dense structure with no obvious porosity. The inner part has many tiny spaces, and it is called spongy bone. Consistent with the structure of the original bone, it could be mimicked by two parts consisting of an outer part made with PLA/PCL/TiO<sub>2</sub> composites and the inner part which might be filled with soft fibers such as extracellular matrix (e.g. collagen) to build the open micro and nano-fluidic channel system.

## Conclusions

Biocompatible polymers have recently gained attention in the field of biomedical applications. Titanium base alloys have been commonly used for bone replacement procedures due to their biocompatible and the mechanical properties. However, the prosthetics which titanium base alloys present several disadvantages such as stress shielding and recurring pain to the subject [31]. The PLA/PCL composites infused with TiO<sub>2</sub> promise to be a better option for bone replacement and grafting procedures. In the present work, it has been demonstrated that Modified Fused Deposition Modeling is suitable for 3D printing

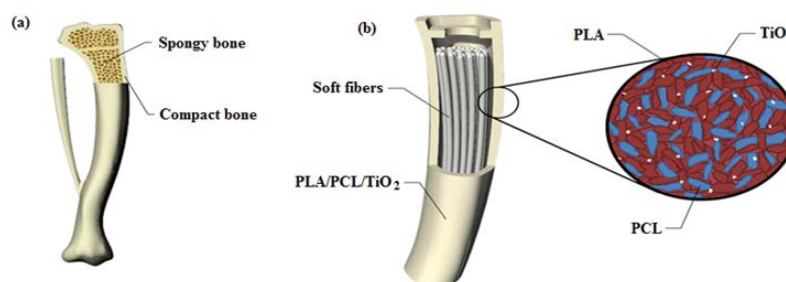


**Figure 11:** (a) Original bone structure, (b) Schematic design of artificial cancellous bone structure with PLA/PCL/TiO<sub>2</sub> and soft fibers.

multifunctional structures for artificial cancellous bone that have been difficult to manufacture with conventional methods. Mechanical properties of PLA/PCL/TiO<sub>2</sub> composites have similar properties to the cancellous bone which were acquired by optimization of the ratio with 3:1 of immiscible PLA/PCL. The strength of PLA/PCL composite presents approximately 30 MPa and the addition of 1 wt.% of TiO<sub>2</sub> particles resulted in an increase of tensile strength up to 37 MPa due to the formation of an interface binding force among PLA, PCL and TiO<sub>2</sub>. By adding this filler, the property of tensile stress has become similar to the cancellous bone (10-50 MPa) [32]. The effect of the total interface area has been studied indicating the optimum results with the maximum interface area making the melt blended composite for creating 3D printed bone structures.

In summary, the PLA/PCL/TiO<sub>2</sub> composite which mimics the cancellous bone was successfully printed using FDM and excellent *in vitro* biocompatibility of composites was demonstrated in this study. Furthermore, the biocompatibility and degradable properties might be enhanced through the addition of a soft filler such as component of extracellular matrix bearing with hydroxyapatite and alginate [33,34].

#### Acknowledgements

This work was supported by the National Research Council of Science and Technology (NST) grant by the Korea government (MSIP) (No. CRC-15-03-KIMM). The authors would like to thank Alan Esparza from the Department of Mechanical Engineering at The University of Texas at El Paso, USA for his assistance in the performance of DSC measurements.

#### Conflicts of Interest

The authors declare no conflict of interest. All intellectual property rights regarding the concept of artificial bone structure using soft fibers are under Printing Nano Engineering Laboratory.

#### References

- Witte F (2015) Reprint of: The history of biodegradable magnesium implants: A review. *Acta Biomater* 23: S28-S40.
- Brydone S, Meek D, MacLaine S (2010) Bone grafting, orthopaedic biomaterials, and the clinical need for bone engineering. *Proc Inst Mech Eng H* 224: 1329-1343.
- Choi K, Kuhn JL, Ciarrelli MJ, Goldstein SA (1990) The elastic moduli of human subchondral, trabecular, and cortical bone tissue and the size-dependency of cortical bone modulus. *J Biomech* 23: 1103-1113.
- Yeni YN, Brown CU, Wang Z, Norman TL (1997) The influence of bone morphology on fracture toughness of the human femur and tibia. *Bone* 21: 453-459.
- Hollister SJ (2005) Porous scaffold design for tissue engineering. *Nat Mater* 4: 518-524.
- Klawitter JJ, Hulbert SF (1971) Application of porous ceramics for the attachment of load bearing internal orthopedic applications. *J Biomed Mater Res* 5: 161-229.
- Sansone V, Pagani D, Melato M (2013) The effects on bone cells of metal ions released from orthopaedic implants. A review. *Clin Cases Miner Bone Metab* 10: 34-40.
- Brar HS, Platt MO, Sarntinoranont M, Martin PI, Manuel MV (2009) Magnesium as a biodegradable and bioabsorbable material for medical implants. *JOM* 61: 31-34.
- Tan L, Yu X, Wan P, Yang K (2013) Biodegradable Materials for Bone Repairs: A Review. *J Mater Sci Technol* 29: 503-513.
- Williams DF (2009) On the nature of biomaterials. *Biomaterials* 30: 5897-5909.
- Place ES, George JH, Williams CK, Stevens MM (2009) Synthetic polymer scaffolds for tissue engineering. *Chem Soc Rev* 38: 1139-1151.
- Cheng Y, Deng S, Chen P, Ruan R (2009) Polylactic acid (PLA) synthesis and modifications: a review. *Front Chem China* 4: 259-264.
- Bolland BJRF, Kanczler JM, Ginty PJ, Howdle SM, Shakesheff KM, et al. (2008) The application of human bone marrow stromal cells and poly(DL-lactic acid) as a biological bone graft extender in impaction bone grafting. *Biomaterials* 29: 3221-3227.
- Wen X, Tresco PA (2006) Fabrication and characterization of permeable degradable poly(DL-lactide-co-glycolide) (PLGA) hollow fiber phase inversion membranes for use as nerve tract guidance channels. *Biomaterials* 27: 3800-3809.
- Halász K, Csóka L (2012) Plasticized biodegradable poly (lactic acid) based composites containing cellulose in micro-and nanosize. *J Eng* 2013.
- Santosh M, Karuppudaiyan VS, Eshraghi S, Das S, Ilankeeran PK, et al. (2011) Mechanical & Microstructural Properties of PCL Scaffolds with 1-D, 2-D & 3-D Orthogonally Oriented Porous Architectures Produced by Selective Laser Sintering. *Acta Biomater* 6: 2467-2476.
- Govor E, Oceli V, Slouf M, Šitum A (2014) Characterization of Biodegradable Polycaprolactone Containing Titanium Dioxide Micro 8: 577-581.
- Zhang J, Song W, Guo J, Zhang J, Sun Z, et al. (2013) Cytotoxicity of different sized TiO<sub>2</sub> nanoparticles in mouse macrophages. *Toxicology and Industrial Health* 29: 523-533.
- Hamzeh M, Sunahara GI (2013) In vitro cytotoxicity and genotoxicity studies of titanium dioxide (TiO<sub>2</sub>) nanoparticles in Chinese hamster lung fibroblast cells. *Toxicology in Vitro* 27: 864-873.
- Visai L, De Nardo L, Punta C, Melone L, Cigada A, et al. (2011) Titanium oxide antibacterial surfaces in biomedical devices. *International Journal of Artificial Organs* 34: 929-946.
- Mofokeng JP, Luyt AS (2015) Morphology and thermal degradation studies of melt-mixed poly(hydroxybutyrate-co-valerate) (PHBV)/poly(caprolactone) (PCL) biodegradable polymer blend nanocomposites with TiO<sub>2</sub> as filler. *J Mater Sci* 50: 3812-3824.
- Sperling LH (1995) Polymer Surfaces and Interfaces: The Need for Uniform Terminology. *ACS Div Polym Mater Sci Eng*.
- Helfand E, Tagami Y (1972) Theory of the Interface Between Immiscible Polymers. *J Chem Phys* 56: 3592.
- Ibrahim BA, Kadum KM (2010) Influence of polymer blending on mechanical and thermal properties. *Modern Applied Science* 4: 157.



25. Khoshkava VKMR, Kamal MR (2013) Effect of surface energy on dispersion and mechanical properties of polymer/nanocrystalline cellulose nanocomposites. *Biomacromolecules* 14: 3155-3163.
26. Wachirahuttapong S, Thongpin C, Sombatsompop N (2016) Effect of PCL and compatibility contents on the morphology, crystallization and mechanical properties of PLA/PCL blends. *Energy Procedia* 89: 198-206.
27. Saeidlou S, Huneault MA, Li H, Park CB (2012) Poly (lactic acid) crystallization. *Progress in Polymer Science* 37: 1657-1677.
28. Harris AM, Lee EC (2008) Improving mechanical performance of injection molded PLA by controlling crystallinity. *Journal of Applied Polymer Science* 107: 2246-2255.
29. Santiago-Medina P, Sundaram PA, Diffoot-Carlo N (2015).Titanium oxide: a bioactive factor in osteoblast differentiation. *International Journal of Dentistry*.
30. Pullisaar H, Tiainen H, Landin MA, Lyngstadaas SP, Haugen HJ, et al. (2013) Enhanced in vitro osteoblast differentiation on TiO<sub>2</sub> scaffold coated with alginate hydrogel containing simvastatin. *Journal of tissue engineering* 4: 2041731413515670.
31. Besinis A, De Peralta T, Handy RD (2012) The antibacterial effects of Ag, TiO<sub>2</sub> and SiO<sub>2</sub> nanoparticles compared to the Dental Disinfectant Chlorhexidine on *Streptococcus mutans* Using a Suite of Bioassays., *Nanotoxicology* 8: 1-45.
32. Hospital AN (1991) Tensile and Compressive Properties of Cancellous Bone. *J Biomech* 24: 1143-1149.
33. Bayrak A, Tyralla M, Ladhoff J, Schleicher M, Stock UA, et al. (2010) Human immune responses to porcine xenogeneic matrices and their extracellular matrix constituents in vitro. *Biomaterials* 31: 3793-3803.
34. Badylak SF (2007) The extracellular matrix as a biologic scaffold material. *Biomaterials* 28: 3587-3593.